Marked improvement in electroluminescence characteristics of organic light-emitting diodes using an ultrathin hole-injection layer of molybdenum oxide

Toshinori Matsushima, Guang-He Jin, and Hideyuki Murata[a)]
School of Materials Science, Japan Advanced Institute of Science and Technology, 1-1 Asahidai, Nomi, Ishikawa 923-1292, Japan

(Received 25 May 2008; accepted 26 June 2008; published online 2 September 2008)

We show that the performance of organic light-emitting diodes (OLEDs) is markedly improved by optimizing the thickness of a hole-injection layer (HIL) of molybdenum oxide (MoO_3) inserted between indium tin oxide and N,N'-diphenyl-N,N'-bis(1-naphthyl)-1,1′-biphenyl-4,4′-diamine (α-NPD). From results of the electroluminescence (EL) characteristics of OLEDs with various thicknesses of a MoO_3 HIL, we found that the OLED with a 0.75-nm-thick MoO_3 HIL had the lowest driving voltage and the highest power conversion efficiency among the OLEDs. Moreover, the operational lifetime of the OLED was improved by about a factor of 6 by using the 0.75-nm-thick MoO_3 HIL. These enhanced EL characteristics are attributable to the formation of an Ohmic contact at the interfaces composed of ITO/MoO_3/α-NPD. © *2008 American Institute of Physics*. [DOI: 10.1063/1.2974089]

I. INTRODUCTION

In recent years, organic light-emitting diodes (OLEDs) have been intensively studied due to their possible applications for low-cost, flexible, large area, lightweight lightings, and displays.[1,2] The practical applications of OLEDs require devices, which have a high power conversion efficiency together with long-term operational stability. To improve the power conversion efficiency and the stability, a reduction in driving voltage is crucial. To reduce the driving voltage, an organic or inorganic hole-injection layer (HIL) has been frequently used between an indium tin oxide (ITO) anode layer and an organic hole-transport layer (HTL) owing to a reduction in hole-injection barrier height.[3–30] Molybdenum oxide (MoO_3) is a material frequently used as a HIL between an ITO layer and a HTL.[5,7,8,12,13,18,19,21,22,24,27,28,30] Also, MoO_3 is used as a *p*-type dopant in a HTL to reduce the driving voltage.[31–34] The thickness of a MoO_3 HIL inserted between an ITO layer and a HTL of N,N'-diphenyl-N,N'-bis(1-naphthyl)-1,1′-biphenyl-4,4′-diamine (α-NPD) was generally greater than 5 nm. Using current density-voltage characteristics of hole-only α-NPD devices with various thicknesses of a MoO_3 HIL, we recently demonstrated that the use of a 0.75-nm-thick MoO_3 HIL inserted between the ITO and the α-NPD only leads to the formation of an Ohmic contact at the ITO/MoO_3/α-NPD interfaces due to electron transfers from ITO to MoO_3 and from α-NPD to MoO_3.[22] This MoO_3 thickness of 0.75 nm is much thinner than the previously reported values and it is crucial to the formation of the Ohmic contact. Since the reduction in hole-injection barrier height improves the stability of OLEDs,[4,24,31,34] the formation of this Ohmic contact not only provides the lowest driving voltage but is also expected to improve the stability of OLEDs. In this study, we investigated how the thickness of a MoO_3 HIL inserted between the ITO and the α-NPD affects the performance of OLEDs. We found that the optimized thickness of a MoO_3 HIL in our OLEDs was 0.75 nm, which is in good agreement with the value obtained in the hole-only devices.[22] The OLED with a 0.75-nm-thick MoO_3 HIL exhibited the lowest driving voltage, the highest power conversion efficiency, and the longest operational lifetime when compared to the OLEDs with other MoO_3 thicknesses. The origin of the enhanced device performance at the particular MoO_3 thickness was discussed.

II. EXPERIMETAL

We fabricated the OLEDs with various thicknesses of a MoO_3 HIL [Fig. 1(a)] according to the following steps. Glass substrates (a size of 25×25 mm^2) coated with an ITO layer (150 nm) with a sheet resistance of 10 Ω/sq (SLR grade, Sanyo Vacuum Industries) were used as a hole-injecting anode. The substrates were cleaned using the procedures, which included ultrasonication in acetone, in detergent, in pure water, and in isopropanol, and finally ultraviolet light irradiation in an ultraviolet-ozone treatment chamber. The cleaned substrates were set in a vacuum evaporator, which was evacuated to around 3×10^{-4} Pa. Under this pressure, a MoO_3 HIL (X nm), an α-NPD HTL (60 nm),[4] an emitting electron-transport layer (ETL) of tris(8-hydroxyquinoline) aluminum (Alq_3) (65 nm),[35] an electron-injection layer of LiF (0.5 nm),[36] and an Al cathode layer (100 nm) were successively vacuum deposited on the ITO anode layer. The thickness of the MoO_3 HIL (X nm) was varied from 0 to 10 nm. The deposition rates were precisely controlled at 0.05 nm/s for MoO_3, 0.1 nm/s for α-NPD and Alq_3, 0.01 nm/s for LiF, and 0.5 nm/s for Al using a quartz crystal microbalance. The active area of the OLEDs was defined by the overlapped area of the ITO and the Al. Four OLEDs with an area of 2×2 mm^2 were prepared on the glass substrate with a size of

a)Electronic mail: murata-h@jaist.ac.jp.

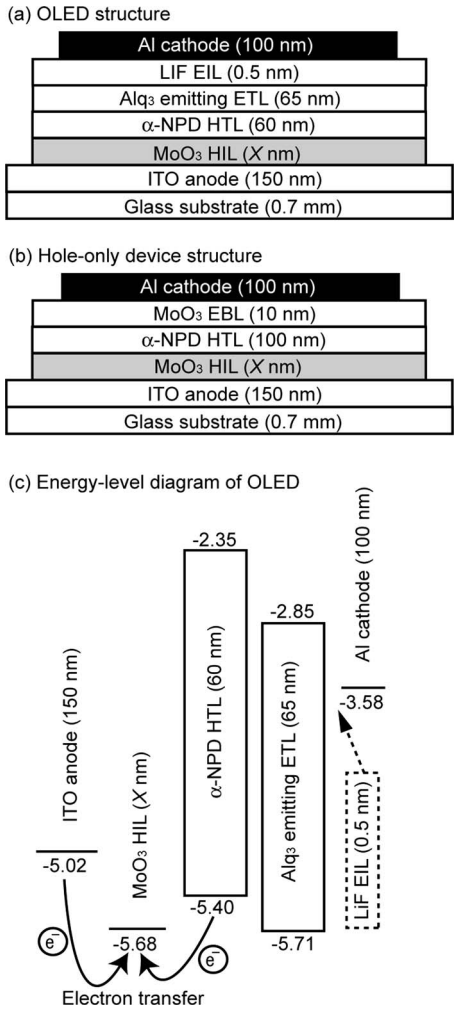

FIG. 1. Schematic structures of (a) OLEDs and (b) hole-only α-NPD devices with various thicknesses (X nm) of MoO_3 HIL and (c) energy-level diagram of OLEDs before making contact between each layer. The thickness (X nm) of MoO_3 HIL inserted between ITO and α-NPD was varied from 0 to 10 nm.

25×25 mm^2. High-purity source materials of MoO_3 (6-N grade, Mitsuwa Chemicals), α-NPD (NN60615, Nippon Steel Chemical), Alq_3 (NA30516, Nippon Steel Chemical), LiF (206–30, Nacalai Tesque), and Al (AL-011480, Nilaco) were purchased and used as received. The completed OLEDs were transferred to a nitrogen-filled glovebox (O_2 and H_2O concentration levels less than 2 ppm) connected to the vacuum evaporator without exposing the OLEDs to ambient air. The OLEDs were encapsulated with a glass cap using an ultraviolet curing epoxy resin inside the glovebox. The current density-voltage-external quantum efficiency characteristics of the OLEDs were measured using a semiconductor characterization system (4200, Keithley Instruments) and an integrating sphere installed with a calibrated silicon photodiode. The glass substrate was placed on a surface of the integrating sphere. Light emitted from the substrate surface was introduced through an aperture (a diameter of 10 mm) into the integrating sphere to eliminate the light emitted from the edge of the glass substrate. The luminance and the power conversion efficiencies of the OLEDs were measured in the direction perpendicular to the substrate surface using a luminance meter (BM-9, TOPCON). To evaluate the operational stability, the times at which the luminance reduced to 90% of their initial luminance (90% lifetimes) of the OLEDs were measured at a constant dc density of 50 mA/cm^2. All measurements were conducted at room temperature.

To investigate the hole-injection characteristics at the ITO/MoO_3/α-NPD interfaces, we fabricated the hole-only α-NPD devices with various thicknesses of a MoO_3 HIL [Fig. 1(b)] using the preparation conditions similar to those previously described. To prevent electron injection from the Al cathode, we used a MoO_3 electron-blocking layer (EBL) with a high work function of -5.68 ± 0.03 eV (Ref. 22) between the α-NPD and the Al. In fact, we observed no electroluminescence (EL) from the devices, meaning that only holes were injected in the devices. The current density-voltage characteristics of the hole-only devices were measured using a semiconductor characterization system (4200, Keithley Instruments) at room temperature.

Thin layers of α-NPD, Alq_3, MoO_3, and Al were prepared on a glass substrate coated with an ITO layer (150 nm) using the same preparation conditions mentioned above. The thickness of all layers was 100 nm. Their ionization potential and work function energy levels were measured by using photoelectron spectroscopy (AC-2, Riken Keiki). We estimated the electron affinity energy levels of the layers of α-NPD and Alq_3 by subtracting their optical absorption onset energy levels from the measured ionization potential energy levels. The energy-level diagram of the OLED is depicted in Fig. 1(c).

III. RESULTS AND DISCUSSION

A. Characteristics of OLEDs with various thicknesses of a MoO_3 HIL

We observed a marked reduction in driving voltage of the OLEDs by using a 0.75-nm-thick MoO_3 HIL. The current density-voltage characteristics of the OLEDs with various MoO_3 thicknesses are shown in Fig. 2(a). The driving voltages of the OLEDs at current densities of 1, 10, and 100 mA/cm^2 are plotted as a function of the MoO_3 thickness in Fig. 2(b). The driving voltages at a certain current density decreased as the MoO_3 thickness was increased from 0 to 0.75 nm. The OLED with the 0.75-nm-thick MoO_3 HIL had the lowest driving voltage among the devices. On the contrary, the driving voltages increased as increasing the MoO_3 thickness from 0.75 to 2 nm. The driving voltages were nearly unchanged in the MoO_3 thickness ranging from 2 to 10 nm. The driving voltage of the OLED with the 0.75-nm-thick MoO_3 HIL was $\approx$7.0 V at a current density of 100 mA/cm^2, which is higher than that of an OLED with a chemically doped HTL (Ref. 6) but lower than those of conventional undoped OLEDs.[3,4,10]

From the results of x-ray photoelectron and ultraviolet/visible/near-infrared absorption studies,[22] we previously found that electron transfers occur from ITO to MoO_3 and from α-NPD to MoO_3. These electron transfers are expected to induce the shift of the Fermi levels of MoO_3 and ITO and the hole-transport level of α-NPD. When the MoO_3 thickness is 0.75 nm, these energy levels are matched and an

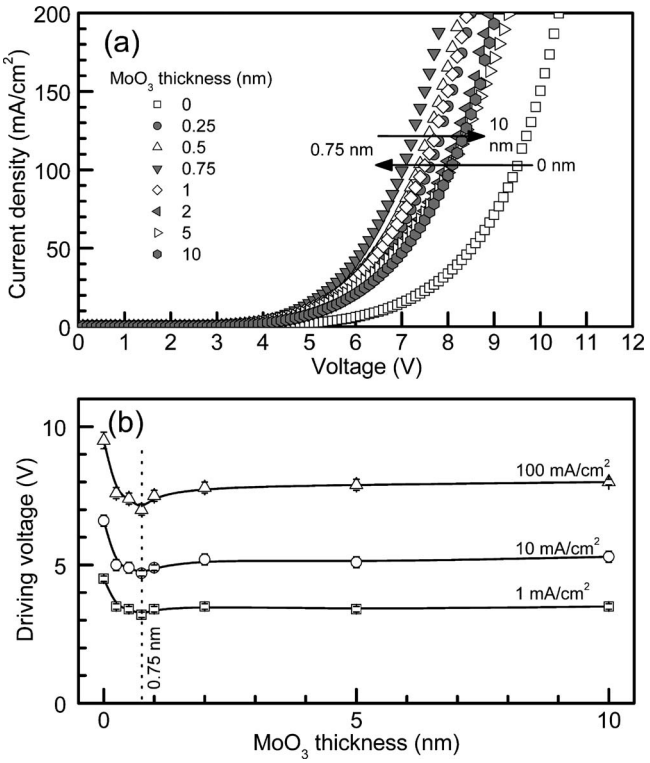

FIG. 2. (a) Current density-voltage characteristics of OLEDs with various thicknesses of MoO_3 HIL and (b) driving voltage at current densities of 1, 10, and 100 mA/cm^2 vs MoO_3 thickness of OLEDs.

Ohmic contact is formed at the interfaces, resulting in the lowest driving voltage observed in the OLED with the 0.75-nm-thick MoO_3 HIL. On the other hand, a strong interfacial dipole layer (IDL), i.e., negatively charged MoO_3 and positively charged α-NPD, is gradually formed at the MoO_3/α-NPD interface as the MoO_3 thickness is increased from 1 to 2 nm. This IDL may lower a hole-injection efficiency and increase the driving voltages of the OLEDs.[37–45]

In all OLEDs, we observed green EL originating from electrically excited Alq_3 molecules. The shapes and the peak tops (528 ± 2 nm) of EL spectra of the OLEDs were consistent with those previously reported[4,9,17] and they were almost independent of both operational current densities ranging from 1 to 100 mA/cm^2 and MoO_3 thickness ranging from 0 to 10 nm. However, the thickness of the MoO_3 HIL inserted between the ITO and the α-NPD markedly affected the external quantum efficiencies and the power conversion efficiencies of the OLEDs. The external quantum efficiencies and the power conversion efficiencies at current densities of 1, 10, and 100 mA/cm^2 are plotted as a function of the MoO_3 thicknesses in Figs. 3 and 4, respectively. The maximum external quantum efficiency of the OLED without MoO_3 was 1.1% at a current density of 66 mA/cm^2, which is in good agreement with those of previously reported OLEDs with an Alq_3 emitter.[46–48] However, the external quantum efficiencies decreased when the MoO_3 HIL was used (Fig. 3). The decrease in the external quantum efficiency is ascribed to an excess number of injected holes in the Alq_3 ETL (Ref. 49) and/or exciton quenching by accumulated holes at the α-NPD/Alq_3 interface,[50,51] resulting from enhanced hole injection from the ITO/MoO_3 contacts.

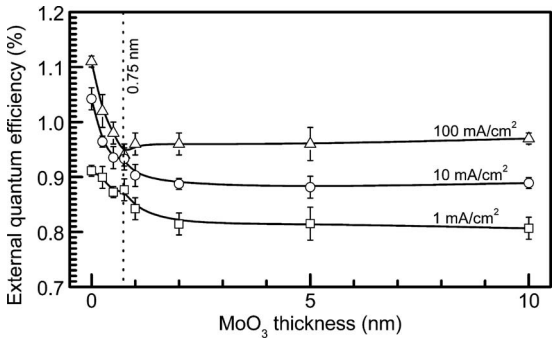

FIG. 3. External quantum efficiency at current densities of 1, 10, and 100 mA/cm^2 vs MoO_3 thickness of OLEDs.

Furthermore, since the marked decrease in the driving voltage (Fig. 2) overcomes the decrease in the external quantum efficiency (Fig. 3), the power conversion efficiencies increased by using the MoO_3 HIL (Fig. 4).

The operational lifetimes of the OLEDs were markedly dependent upon the MoO_3 thickness. The luminance/initial luminance-time characteristics of the OLEDs were measured at a constant dc density of 50 mA/cm^2 at room temperature [Fig. 5(a)]. The initial luminance at 50 mA/cm^2 was about 1500 cd/m^2, which was slightly changed depending upon the MoO_3 thickness. The 90% lifetimes of the OLEDs are plotted as a function of the MoO_3 thickness in Fig. 5(b). The OLED with the 0.75-nm-thick MoO_3 HIL had the longest 90% lifetime (190 h) among the OLEDs investigated in this study. By fitting the experimental luminance decay curve of this OLED with a stretched single exponential equation,[52] the time at which the luminance reached half of the initial luminance (half lifetime) was estimated to be approximately 3200 h at a current density of 50 mA/cm^2 (an initial luminance of 1440 cd/m^2). This value lies above half lifetimes of previously reported OLEDs with an Alq_3 emitter operated under the similar conditions.

The luminance of the OLED without MoO_3 suddenly decreased at the initial stage (<10 h) of the device operation [Fig. 5(a)]. However, the insertion of the MoO_3 HIL between the ITO and the α-NPD drastically suppressed this initial degradation. The OLED with the 0.75-nm-thick MoO_3 HIL exhibited no initial degradation and had an about six times longer 90% lifetime (190 h) than the OLED without MoO_3 (32 h). This result manifests that this initial degradation occurs near the ITO/α-NPD interface. The origin of the initial

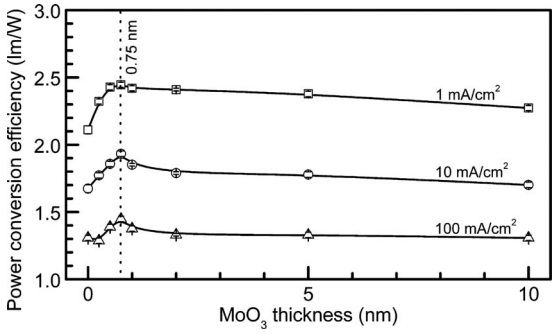

FIG. 4. Power conversion efficiency at current densities of 1, 10, and 100 mA/cm^2 vs MoO_3 thickness of OLEDs.

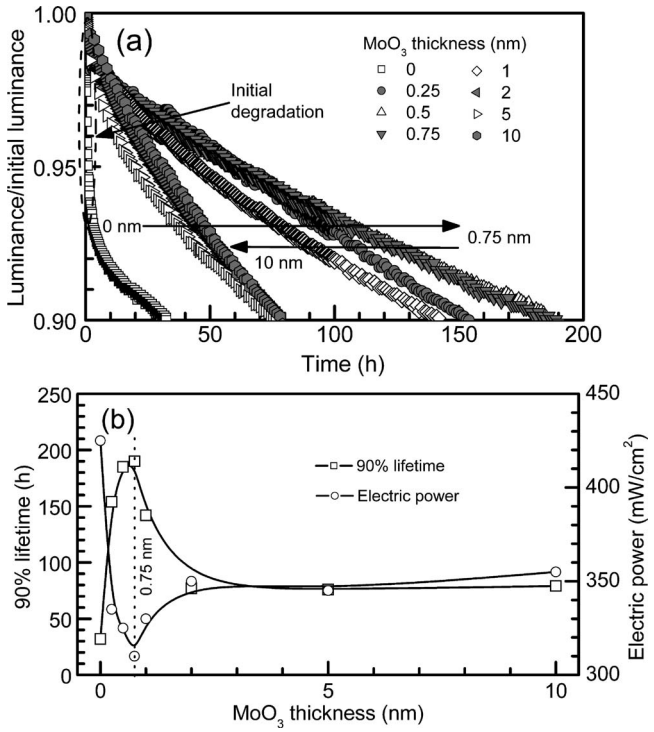

FIG. 5. (a) Luminance/initial luminance-time characteristics of OLEDs with various thickness of MoO_3 HIL and (b) 90% lifetime and electric power vs MoO_3 thickness of OLEDs. All OLEDs were operated at constant dc current density of 50 mA/cm^2.

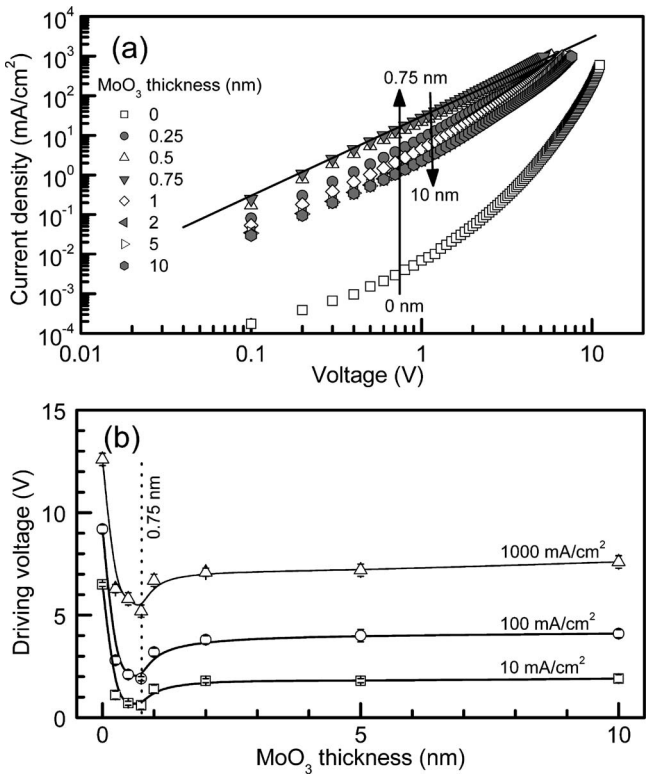

FIG. 6. (a) Current density-voltage characteristics of hole-only α-NPD devices with various thickness of MoO_3 HIL and (b) driving voltage at current densities of 10, 100, and 1000 mA/cm^2 vs MoO_3 thickness of hole-only α-NPD devices. Solid line in (a) represents SCLC expressed as $J=(9/8)\varepsilon_r\varepsilon_0\mu_{\text{eff}}(V^2/L^3)$, where J is current density, ε_r is relative permittivity (3.0), ε_0 is vacuum permittivity (8.845×10^{-12} F/m), μ_{eff} is carrier mobility ($1.0\pm0.1\times10^{-4}$ cm^2/V s), V is voltage, and L is cathode-anode spacing (100 nm). (Ref. 22)

degradation might be attributed to the migration of indium components into the α-NPD HTL (Refs. 53 and 54) and/or a chemical reaction between the α-NPD and hydroxyl groups on the ITO surface.[55]

We would like to point out that after the initial degradation, all OLEDs exhibited the gradual decrease in luminance [Fig. 5(a)]. The electric power (E) consumed by the operation of the OLEDs is expressed as an equation $E=JV$, where J is the current density and V is the driving voltage. The calculated electric powers of the OLEDs operated at 50 mA/cm^2 are also plotted in Fig. 5(b). We found that the OLEDs with lower electric powers have longer operational lifetimes. This result indicates that the OLED degradation is related to Joule heat generated inside the OLEDs and it is consistent with the fact that operating OLEDs under a higher bias voltage at a higher temperature accelerates the degradation of OLEDs,[56–59] indicating that the device degradation may rapidly proceed under high temperature conditions. Since electrochemically decomposed species act as nonradiative recombination centers and/or luminance quenchers in a carrier recombination zone, EL efficiencies of OLEDs gradually decrease as the amount of decomposed species increases with operational time.[60–62] The incorporation of H_2O molecules into the Alq_3 emitting layer during its evaporation has been shown to induce an electrochemical decomposition of Alq_3.[63] From these considerations, we assume that the long-term degradation of the OLEDs originates from a thermally induced electrochemical decomposition of organic molecules. Decreasing the driving voltages (electric powers) may reduce a temperature increase inside the OLEDs and the probability of a thermally induced degradation process of the OLEDs.

B. Characteristics of hole-only devices with various thickness of a MoO_3 HIL

To obtain more detailed information on the change in the current density-voltage characteristics shown in Fig. 2(a), we analyzed hole-only α-NPD devices, whose structure is shown in Fig. 1(b). The current density-voltage characteristics of the hole-only devices are shown in Fig. 6(a). The driving voltages of the hole-only devices at current densities of 10, 100, and 1000 mA/cm^2 are plotted as a function of the MoO_3 thickness in Fig. 6(b). The hole-only device with the 0.75-nm-thick MoO_3 HIL exhibited the highest current density and a square law. These observations indicate that the current density-voltage characteristics of this device are controlled by a space-charge-limited current (SCLC) mechanism [solid line in Fig. 6(a)] and that an Ohmic contact is formed at the ITO/MoO_3(0.75 nm)/α-NPD interfaces. Details of these characteristics of the hole-only devices have been discussed in Ref. 22. Since the driving voltages of the hole-only devices [Fig. 6(b)] were changed in a manner similar to the driving voltages of the OLEDs [Fig. 2(b)], we conclude that the improved OLED performance discussed in Sec. III A was ascribed to the enhanced hole injection from the ITO/MoO_3 anodes.

The MoO_3 layers with various thicknesses were prepared on a glass substrate coated with an ITO layer. The work functions of these samples were measured using AC-2 pho-

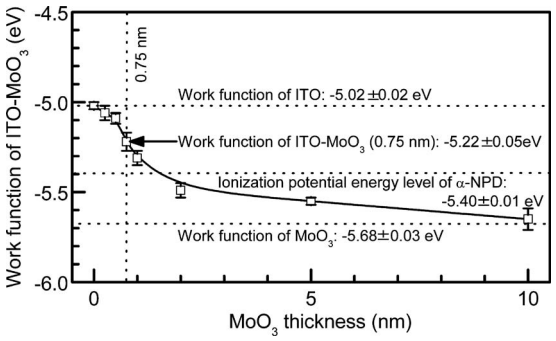

FIG. 7. Work functions of glass/ITO (150 nm)/MoO_3(X nm) samples as a function of MoO_3 thickness (X nm). The thickness (X nm) of MoO_3 layer on ITO was varied from 0 to 10 nm.

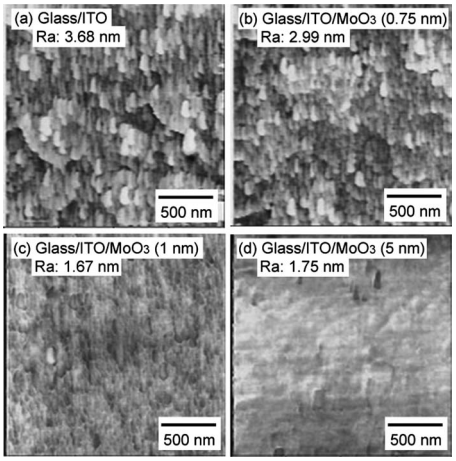

FIG. 8. Atomic force microscope images of glass/ITO (150 nm)/MoO_3(X nm) samples: (a) $X=0$ nm, (b) $X=0.75$ nm, (c) $X=1$ nm, and (d) $X=5$ nm.

toelectron spectroscopy. The relationship between the work functions of the ITO/MoO_3 anodes and the MoO_3 thickness is shown in Fig. 7. The work functions of the ITO/MoO_3 anodes markedly increased as the MoO_3 thickness was increased from 0 to 2 nm due to an electron transfer from ITO to MoO_3.[22] When the MoO_3 thickness was increased from 2 to 10 nm, the work functions of the ITO/MoO_3 anodes gradually approached the work function level of an intrinsic MoO_3 layer (-5.68 ± 0.03 eV) (Ref. 22). At the MoO_3 thickness of 0.75 nm, the ITO/MoO_3 anode had a work function of -5.22 ± 0.05 eV, indicating that a hole-injection barrier (≈ 0.18 eV) was still present at the anode/α-NPD interface. It should be noted that this hole-injection barrier height (≈ 0.18 eV) was calculated from the difference in energy level between the work function of the ITO/MoO_3 layer (-5.22 ± 0.05 eV) and the ionization potential energy level of an intrinsic α-NPD layer (-5.40 ± 0.01 eV) (Ref. 22) before these layers were in contact. As mentioned in the Sec. III A, we confirmed that electron transfers occur both from ITO to MoO_3 and from α-NPD to MoO_3 [see Fig. 1(c)].[22] The electron transfer from α-NPD to MoO_3 induces an increase in free hole concentration in the α-NPD HTL near the MoO_3/α-NPD interface. This increase in free hole concentration leads to matching between the Fermi level of the ITO/MoO_3 anode layer and the hole transport level of the α-NPD layer,[64,65] resulting in the formation of the Ohmic contact at the interfaces. We would like to emphasize again that the double electron transfers from ITO to MoO_3 and from α-NPD to MoO_3 are indispensable to the formation of the Ohmic contact.

The morphologies of the ITO/MoO_3 surfaces were measured using an atomic force microscope (SPA400, Seiko Instruments). The results are shown in Fig. 8. When the MoO_3 thicknesses were 0 and 0.75 nm, the ITO/MoO_3 surfaces had a relatively large grain structure with a large average surface roughness [Figs. 8(a) and 8(b)]. As the MoO_3 thickness was increased from 1 to 5 nm, the grain structures gradually disappeared and the ITO/MoO_3 surfaces became flat [Figs. 8(c) and 8(d)], suggesting that the ITO surface was probably covered with the MoO_3 layer. In this case, depositing the α-NPD on the flat ITO/MoO_3 surfaces would form a strong IDL which may impede the hole injection at the interface. To clarify a detailed mechanism of the IDL formation is an interesting research topic and we are now investigating to elucidate the mechanism.

IV. CONCLUSIONS

We investigated how the thickness of a MoO_3 HIL inserted between an ITO anode and an α-NPD HTL influences EL characteristics of OLEDs and hole-injection characteristics of hole-only α-NPD devices. We found the optimized MoO_3 thickness to be 0.75 nm, which provided the lowest driving voltage, the highest power conversion efficiency, and the longest lifetime for the OLED. Moreover, current density-voltage characteristics of the hole-only α-NPD device with the 0.75-nm-thick MoO_3 HIL were controlled by a SCLC mechanism, indicating that an Ohmic contact was formed at the ITO/MoO_3(0.75 nm)/α-NPD interfaces. The formation of the Ohmic contact using the 0.75-nm-thick MoO_3 HIL was ascribed to (1) an electron transfer from ITO to MoO_3, (2) an electron transfer from α-NPD to MoO_3, and (3) incomplete coverage of an ITO surface by MoO_3. Finally, we emphasize that the findings presented in this study are valuable in developing organic (opto)electronic devices as well as clarifying the underlying mechanisms of carrier transport in organic films.

ACKNOWLEDGMENTS

We thank the New Energy and Industrial Technology Development Organization (NEDO) of Japan for financial support of this work.

[1] S. R. Forrest, Nature (London) **428**, 911 (2004).
[2] N. Koch, ChemPhysChem **8**, 1438 (2007).
[3] Y. Shirota, Y. Kuwabara, H. Inada, T. Wakimoto, H. Nakada, Y. Yonemoto, S. Kawami, and K. Imai, Appl. Phys. Lett. **65**, 807 (1994).
[4] S. A. Van Slyke, C. H. Chen, and C. W. Tang, Appl. Phys. Lett. **69**, 2160 (1996).
[5] S. Tokito, K. Noda, and Y. Taga, J. Phys. D **29**, 2750 (1996).
[6] X. Zhou, M. Pfeiffer, J. Blochwitz, A. Werner, A. Nollau, T. Fritz, and K. Leo, Appl. Phys. Lett. **78**, 410 (2001).
[7] K. J. Reynolds, J. A. Barker, N. C. Greenham, R. H. Friend, and G. L. Frey, J. Appl. Phys. **92**, 7556 (2002).
[8] G. L. Frey, K. J. Reynolds, and R. H. Friend, Adv. Mater. (Weinheim,

Ger.) **14**, 265 (2002).
[9]T. Dobbertin, M. Kroeger, D. Heithecker, D. Schneider, D. Metzdorf, H. Neuner, E. Becker, H.-H. Johannes, and W. Kowalsky, Appl. Phys. Lett. **82**, 284 (2003).
[10]S.-F. Chen and C.-W. Wang, Appl. Phys. Lett. **85**, 765 (2004).
[11]Y. Kim, K. H. Bae, Y. Y. Jeong, D. K. Choi, and C.-S. Ha, Chem. Mater. **16**, 5051 (2004).
[12]C.-W. Chen, Y.-J. Lu, C.-C. Wu, E. H.-E. Wu, C.-W. Chu, and Y. Yang, Appl. Phys. Lett. **87**, 241121 (2005).
[13]T. Miyashita, S. Naka, H. Okada, and H. Onnagawa, Jpn. J. Appl. Phys., Part 1 **44**, 3682 (2005).
[14]J. Li, M. Yahiro, K. Ishida, H. Yamada, and K. Matsushige, Synth. Met. **151**, 141 (2005).
[15]S. Y. Kim, J. M. Baik, H. K. Yu, and J.-L. Lee, J. Appl. Phys. **98**, 093707 (2005).
[16]T. Matsushima and C. Adachi, Appl. Phys. Lett. **89**, 253506 (2006).
[17]P.-C. Kao, S.-Y. Chu, Z.-X. You, S. J. Liou, and C.-A. Chuang, Thin Solid Films **498**, 249 (2006).
[18]H. Kanno, N. C. Giebink, Y. Sun, and S. R. Forrest, Appl. Phys. Lett. **89**, 023503 (2006).
[19]R. Satoh, S. Naka, M. Shibata, H. Okada, H. Onnagawa, T. Miyabayashi, and T. Inoue, Jpn. J. Appl. Phys., Part 1 **45**, 1829 (2006).
[20]K. Okumoto, H. Kanno, Y. Hamada, H. Takahashi, and K. Shibata, J. Appl. Phys. **100**, 044507 (2006).
[21]J.-H. Li, J. Huang, and Y. Yang, Appl. Phys. Lett. **90**, 173505 (2007).
[22]T. Matsushima, Y. Kinoshita, and H. Murata, Appl. Phys. Lett. **91**, 253504 (2007).
[23]J. Meyer, S. Hamwi, T. Bülow, H.-H. Johannes, T. Riedl, and W. Kowalsky, Appl. Phys. Lett. **91**, 113506 (2007).
[24]H. You, Y. Dai, Z. Zhang, and D. Ma, J. Appl. Phys. **101**, 026105 (2007).
[25]J. Y. Lee, J.-Y. Park, S.-H. Min, K.-W. Lee, and Y. G. Baek, Thin Solid Films **515**, 7726 (2007).
[26]Q. Huang, J. Li, T. J. Marks, G. A. Evmenenko, and P. Dutta, J. Appl. Phys. **101**, 093101 (2007).
[27]H. Zhang, Y. Dai, D. Ma, and H. Zhang, Appl. Phys. Lett. **91**, 123504 (2007).
[28]X.-Y. Jiang, Z.-L. Zhang, J. Cao, M. A. Khan, Khizar-ul-Haq, and W. Q. Zhu, J. Phys. D **40**, 5553 (2007).
[29]J. Jang, J. Ha, and K. Kim, Thin Solid Films **516**, 3152 (2008).
[30]T.-W. Lee, T. Noh, B.-K. Choi, M.-S. Kim, D. W. Shin, and J. Kido, Appl. Phys. Lett. **92**, 043301 (2008).
[31]H. Ikeda, J. Sakata, M. Hayakawa, T. Aoyama, T. Kawakami, K. Kamata, Y. Iwaki, S. Seo, Y. Noda, R. Nomura, and S. Yamazaki, 2006 Society for Information Display International Symposium, Digest of Technical Papers, San Francisco, CA, 2006 (unpublished), p. 923.
[32]T. Matsushima and C. Adachi, J. Appl. Phys. **103**, 034501 (2008).
[33]G. Xie, Y. Meng, F. Wu, C. Tao, D. Zhang, M. Liu, Q. Xue, W. Chen, and Y. Zhao, Appl. Phys. Lett. **92**, 093305 (2008).
[34]W.-J. Shin, J.-Y. Lee, J. C. Kim, T.-H. Yoon, T.-S. Kim, and O.-K. Song, Org. Electron. **9**, 333 (2008).
[35]C. W. Tang and S. A. Van Slyke, Appl. Phys. Lett. **51**, 913 (1987).
[36]L. S. Hung, C. W. Tang, and M. G. Mason, Appl. Phys. Lett. **70**, 152 (1997).
[37]I. H. Campbell, S. Rubin, T. A. Zawodzinski, J. D. Kress, R. L. Martin, D. L. Smith, N. N. Barashkov, and J. P. Ferraris, Phys. Rev. B **54**, R14321 (1996).
[38]S. T. Lee, X. Y. Hou, M. G. Mason, and C. W. Tang, Appl. Phys. Lett. **72**, 1593 (1998).
[39]E. Ito, H. Oji, H. Ishii, K. Oichi, Y. Ouchi, and K. Seki, Chem. Phys. Lett. **287**, 137 (1998).
[40]F. Nüesch, F. Rotzinger, L. Si-Ahmed, and L. Zuppiroli, Chem. Phys. Lett. **288**, 861 (1998).
[41]L. Yan, N. J. Watkins, S. Zorba, Y. Gao, and C. W. Tang, Appl. Phys. Lett. **81**, 2752 (2002).
[42]N. Hayashi, H. Ishii, Y. Ouchi, and K. Seki, J. Appl. Phys. **92**, 3784 (2002).
[43]I.-H. Hong, M.-W. Lee, Y.-M. Koo, H. Jeong, T.-S. Kim, and O.-K. Song, Appl. Phys. Lett. **87**, 063502 (2005).
[44]T. Y. Chu and O. K. Song, Appl. Phys. Lett. **90**, 203512 (2007).
[45]T. Y. Chu and O. K. Song, Appl. Phys. Lett. **91**, 073508 (2007).
[46]G. Sakamoto, C. Adachi, T. Koyama, Y. Taniguchi, C. D. Merritt, H. Murata, and Z. H. Kafafi, Appl. Phys. Lett. **75**, 766 (1999).
[47]K. Okumoto, H. Kanno, Y. Hamada, H. Takahashi, and K. Shibata, Appl. Phys. Lett. **89**, 013502 (2006).
[48]V. V. Jarikov, R. H. Young, J. R. Vargas, C. T. Brown, K. P. Klubek, and L.-S. Liao, J. Appl. Phys. **100**, 094907 (2006).
[49]T. Tsutsui, Mater. Res. Bull. **22**, 39 (1997).
[50]Y. Luo, H. Aziz, G. Xu, and Z. D. Popovic, Chem. Mater. **19**, 2288 (2007).
[51]T. Matsushima and C. Adachi, Appl. Phys. Lett. **92**, 063306 (2008).
[52]C. Féry, B. Racine, D. Vaufrey, H. Doyeux, and S. Cinà, Appl. Phys. Lett. **87**, 213502 (2005).
[53]A. R. Schlatmann, D. W. Floet, A. Hilberer, F. Garten, P. J. M. Smulders, T. M. Klapwijk, and G. Hadziioannou, Appl. Phys. Lett. **69**, 1764 (1996).
[54]S. T. Lee, Z. Q. Gao, and L. S. Hung, Appl. Phys. Lett. **75**, 1404 (1999).
[55]K. Akedo, A. Miura, K. Noda, and H. Fujikawa, Proceedings of the 13th International Display Workshops, 2006 (unpublished), p. 465.
[56]I. D. Parker, Y. Cao, and C. Y. Yang, J. Appl. Phys. **85**, 2441 (1999).
[57]H. Murata, C. D. Merritt, H. Inada, Y. Shirota, and Z. H. Kafafi, Appl. Phys. Lett. **75**, 3252 (1999).
[58]X. Zhou, J. He, L. S. Liao, M. Lu, X. M. Ding, X. Y. Hou, X. M. Zhang, X. Q. He, and S. T. Lee, Adv. Mater. (Weinheim, Ger.) **12**, 265 (2000).
[59]M. Ishii and Y. Taga, Appl. Phys. Lett. **80**, 3430 (2002).
[60]J. C. Scott, J. H. Kaufman, P. J. Brock, R. DiPietro, J. Salem, and J. A. Goitia, J. Appl. Phys. **79**, 2745 (1996).
[61]D. Y. Kondakov, W. C. Lenhart, and W. F. Nichols, J. Appl. Phys. **101**, 024512 (2007).
[62]Y. Luo, H. Aziz, Z. D. Popovic, and G. Xu, J. Appl. Phys. **101**, 034510 (2007).
[63]T. Ikeda, H. Murata, Y. Kinoshita, J. Shike, Y. Ikeda, and M. Kitano, Chem. Phys. Lett. **426**, 111 (2006).
[64]M. Pfeiffer, A. Beyer, T. Fritz, and K. Leo, Appl. Phys. Lett. **73**, 3202 (1998).
[65]J. Blochwitz, T. Fritz, M. Pfeiffer, K. Leo, D. M. Alloway, P. A. Lee, and N. R. Armstrong, Org. Electron. **2**, 97 (2001).